International Conference on Control, Engineering & Information Technology (CEIT'14)
Proceedings - Copyright IPCO-2014. ISSN 2356-5608

Induction Motor Fault Diagnosis Based On the Radial Vibration Analytic Signal

A. Medoued, A. Lebaroud, M. Mordjaoui, D.Sayad
Département de génie électrique, Université du 20 août 1955-Skikda, Algeria
E-mail:amedoud@yahoo.fr; amedoued@ieee.org

***Abstract*— We present a new method of fault diagnosis based on the analysis of the Radial Vibration Analytic Signal (*RVAS*). Calculations are applied to vibration signals generated by a defected bearing of the induction motor. The calculation method consists of two main parts: the first is the Hilbert transform of the radial vibration normalized and compared with the module of the *RVAS*. The second consists of the extraction of feature form vectors using the Signal Class Dependent Time Frequency Representation (TFR_{SCD}). The Fisher contrast is used to design the non parametrical kernel of TFR_{SCD}. The feature vector size is optimized using Particle Swarm Optimization technique (*PSO*). The results are validated on a 5.5-kW induction motor test bench.**

***Key words*—** Induction motor diagnosis, Time-Frequency TFR, PSO, Feature extraction.

I. INTRODUCTION

The field of fault diagnosis is heading towards the development of more reliable and powerful machine health monitoring schemes. Today's industry strives to improve performance and profitability while maintaining and improving safety. Thus, very expensive scheduled maintenance is performed in order to detect machine problems before they may result in catastrophic failures [1]. In this light, several monitoring techniques have been developed to detect induction machine faults. Among all of these, those relying on the examination of the frequency component in the motor current spectrum, called Motor Current Signature Analysis (MCSA) which has gained attention from researchers. Other techniques are based on vibration analysis, acoustic noise measurement, torque profile analysis, temperature analysis, and magnetic field analysis [2]. These techniques require sophisticated and expensive sensors, additional electrical and mechanical installations, and frequent maintenance. In addition to recent techniques based on artificial intelligence approaches such as artificial neural networks [3- 8], fuzzy logic [9], wavelets [10], etc…

Generally, diagnosis systems use signals either in time or frequency domain. In our approach, both time and frequency are combined in order to extract much information about the health condition of the machine.

Time–frequency analysis of the motor current makes signal properties, related to fault detection, more evident in the transform domain [11].

Usually, the objective of time–frequency research is to create a function that represents the energy density of a signal simultaneously in both time and frequency, for classification purpose. It is not necessarily desirable to accurately represent the energy distribution of a signal.

In fact, such a representation may conflict with the goal of classification, generating a TFR that maximizes the separability of TFRs from different classes. It may be advantageous to design TFRs that specifically highlight differences between classes [12-13].

We propose to design and use the classifier directly in the ambiguity Doppler delay plane. Since all TFRs can be derived from the ambiguity plane, no *a priori* assumption is made about the smoothing required for accurate classification. Thus, the smoothing quadratic TFRs retain only the information that is essential for classification.

This classification allows us to proceed to an optimization routine based on particle swarm technique to find the appropriate size of the feature vectors in order to reduce calculation time and keep the signal with relevant information within the vectors.

The classification procedure is based on the design of an optimized TFR from a time–frequency ambiguity plane in order to extract the feature vector. The optimal size of the feature vectors is obtained using PSO algorithm [14]. The PSO technique can generate high-quality solutions within shorter calculation time and stable convergence characteristic than any other stochastic methods [15-16].

The goal of this work is the realization of an accurate diagnosis system based on the analysis of the radial vibration signal caused by bearing faults.

II. Hilbert transform of Radial vibrations

Since we cannot directly use the vibration signals due to their very low values. We present a method for preprocessing before the use of the TFR_{SCD}. The method involves the calculation of a very interesting parameter: the dispersion parameter ξ of the point cloud. It is this parameter that allows the calculation of the TFR_{SCD} and the extraction of the feature vectors.

Radial Vibration Analytic Signal (RVAS) method uses the principle of the analytical signal obtained by Hilbert transform. The Hilbert transform in the time domain corresponds to a $\pi/2$-phase shift of the Fourier

transform terms. Hilbert transform finds a companion function y(t) for a real function x(t) so that :

$z(t) = x(t) + iy(t)$. The Hilbert transform of a signal $x(t)$ can be written as:

$$x(t) \xrightarrow{HT} \tilde{x}(t) = \tilde{x}_{\mathrm{Re}}(t) + j\tilde{x}_{\mathrm{Im}}(t) \quad (1)$$

where $\tilde{x}_{\mathrm{Im}}(t)$ represents the Hilbert transform of the signal $\tilde{x}_{\mathrm{Re}}(t)$. The signal $\tilde{x}(t)$, meanwhile, is commonly called analytic signal.
The amplitude $A(t)$ of the time signal $x(t)$ is calculated using the following relation:

$$A(t) = \sqrt{(\tilde{x}_{\mathrm{Re}}(t))^2 + (\tilde{x}_{\mathrm{Im}}(t))^2} \quad (2)$$

Its phase $\varphi(t)$ is calculated using the relation:

$$\varphi(t) = \arctan\frac{\tilde{x}_{\mathrm{Im}}(t)}{\tilde{x}_{\mathrm{Re}}(t)} \quad (3)$$

Applying this to our case for the radial vibration signal $\mathrm{V_R(t)}$, we get :

$$V_R(t) \xrightarrow{HT} \tilde{V}_R(t) = \tilde{V}_{R\,\mathrm{Re}}(t) + j\tilde{V}_{R\,\mathrm{Im}}(t) \quad (4)$$

Where $\tilde{V}_{R\,\mathrm{Im}}(t)$ represents The Hilbert transform of the Radial vibration signal $\tilde{V}_{R\,\mathrm{Re}}$. And $V_R(t)$ is usually called the Radial Vibration Analytic Signal (RVAS).

The amplitude is:

$$A(t) = \sqrt{\tilde{V}_{R\,\mathrm{Re}}(t)^2 + \tilde{V}_{R\,\mathrm{Im}}(t)^2} \quad (5)$$

The real and imaginary radial vibrations are normalised to the module of the RVAS :

$$\tilde{V}'_{R\,\mathrm{Re}}(t) = \frac{\tilde{V}_{R\,\mathrm{Re}}(t)}{A(t)} \quad (6)$$

$$\tilde{V}'_{R\,\mathrm{Im}}(t) = \frac{\tilde{V}_{R\,\mathrm{Im}}(t)}{A(t)} \quad (7)$$

$$A'(t) = \sqrt{\left[\tilde{V}'_{R\,\mathrm{Re}}(t)\right]^2 + \left[\tilde{V}'_{R\,\mathrm{Im}}(t)\right]^2} \quad (8)$$

The vibrations average is given by:

$$m\tilde{V}'_{R\,\mathrm{Re}} = \frac{1}{N'_{\tilde{V}R}}\sum_{k=1}^{N'_{\tilde{V}a}} \tilde{V}'_{R\,\mathrm{Re}}(k) \quad (9)$$

$$m\tilde{V}'_{R\,\mathrm{Im}} = \frac{1}{N'_{\tilde{V}R}}\sum_{k=1}^{N'_{\tilde{V}a}} \tilde{V}'_{R\,\mathrm{Im}}(k) \quad (10)$$

The normalised characteristic $\tilde{V}'_{R\,\mathrm{Im}}, \tilde{V}'_{R\ \mathrm{Re}}$ consists of a cloud of $N'_{\tilde{V}R}$ points. These points represent in a normalised way the instantaneous evolution of the radial vibrations.

The parameter ξ, that represents the cloud dispersion of these points is defined as :.

$$\xi = \sum_{k=1}^{NvR}(A_k - m\tilde{V}'_{R\,\mathrm{Re}})(A_k - m\tilde{V}'_{R\,\mathrm{Im}})^T \quad (11)$$

Where A_k is a point with coordinates $(\tilde{V}'_{R\,\mathrm{Re}}(k), \tilde{V}'_{R\,\mathrm{Im}}(k))$

The parameter ξ is relatively sensitive to different states of the machine such as defected bearings, broken bars or unbalanced feed.

II. Feature Extraction using TFR

For further details, we recommend the reader to review our previous works [17]-[18].
The characteristic function for each TFR is $A(\eta,\tau)\varphi(\eta,\tau)$, η represents the discrete frequency shift and τ represents the discrete time delay. This means that the optimal-classification representation TFR*i* can be obtained by smoothing the ambiguity plane $A(\eta,\tau)$ with an appropriate kernel φ_{opt}, which is an optimal classification kernel. The problem of designing the TFR*i* becomes equivalent to designing the optimal classification kernel $\varphi_{opt}(\eta,\tau)$. This method, used to design kernels (and thus TFRs), optimizes the discrimination between predefined sets of classes.

Features can be extracted directly from $A(\eta,\tau)\varphi_{opt}(\eta,\tau)$ instead of the optimal classification TFR*i*. This shortcut simplifies the computation complexity of the feature extraction by reducing the calculations.

The $\mathrm{TFR_{SCD}}$ does not allow us to limit the size of the feature vector. To solve this problem we have used the PSO algorithm to minimize the sizes of the feature vectors without affecting the relevance of these vectors.

III. OPTIMIZATION USING PSO ALGORITHM

One objective of our approach is to minimize the size of the signal by a feature vector of a very small size without losing relevant information of the signal. Hence, an optimum size of this vector provides a good compromise between the relevance of information and time consuming cost. In this work, the size used in the previous calculations is determined using PSO algorithm.

A. Particle Swarm Optimization (PSO)

The main advantages of PSO algorithm are summarized as: simple concept, easy implementation, robustness to control parameters, and computational efficiency when compared with mathematical algorithms and other heuristic optimization techniques. In PSO, two different definitions are used: the individual best and the global best. As a particle moves through the search space, it compares its fitness value at the current position to the best fitness value it has ever attained previously. The best position that is associated with the best fitness encountered so far is called the individual best or *pbest*. The global best, or *gbest*, is the best position among all of the individual's best positions achieved so far (Fig. 1).
Using the *gbest* and the *pbest*, the i[th] particle velocity is updated according to the following equation [16]:

$$v_i^{k+1} = w v_i^k + c_1 rand_1 \times (pbest_i - s_i^k) + c_2 rand_2 \times (gbest - s_i^k) \quad (12)$$

Based on the updated velocities, each particle changes its position according to the equation:

$$s_i^{k+1} = s_i^k + v_i^{k+1} \quad (13)$$

Where w is a weighting function, c_j are acceleration factors and *rand* is a random number between 0 and 1.
The following weighting function is usually utilized:

$$w = w_{\max} - \frac{w_{\max} - w_{\min}}{iter_{\max}} \times iter \quad (14)$$

Where w_{max} is initial weight, w_{min} the final weight, $iter_{max}$ is the maximum iteration number, and *iter* is the current iteration number.
The parameters used in this work are taken as follows [19-22]:
c_1=c_2=2.05; $w_{\min}$ =0.1; $w_{\max}$ =0.9.

Selection of maximum velocity:

At each iteration step, the algorithm proceeds by adjusting the distance (velocity) that each particle moves in every dimension of the problem hyperspace. The velocity of the particle is a stochastic variable and is, therefore, subject to creating an uncontrolled trajectory, making the particle follow wider cycles in the problem space. In order to damp these oscillations, upper and lower limits can be defined for the velocity v_i :

$$\begin{aligned} &if \quad v_i > v_{\max} \quad then \quad v_i = v_{\max} \\ &elseif \quad v_i < -v_{\max} \quad then \quad v_i = -v_{\max} \end{aligned} \quad (15)$$

Generally, the value of $v_{\max}$ is selected empirically, according to the characteristics of the problem. It is important to note that if the value of this parameter is too large, then the particles may move erratically, going beyond a good solution; on the other hand, if $v_{\max}$ is too small, then the particle's movement is limited and the optimal solution may not be reached.
Research work performed by Fan and Shi [23] have shown that an appropriate dynamically changing $v_{\max}$ can improve the performance of the PSO algorithm. In the simulation part and to ensure a uniform velocity we fixed $v_{\max}$ according to many run tests.

Integer PSO formulation:

In the case where integer variables are included in the optimization problem such as a size of feature vector, the PSO algorithm can be reformulated by rounding off the particle's position to the nearest integer. Mathematically, (12) and (13) are still valid, but once the new particle's position is determined in the real-number space, the conversion to the integer number space must be done.

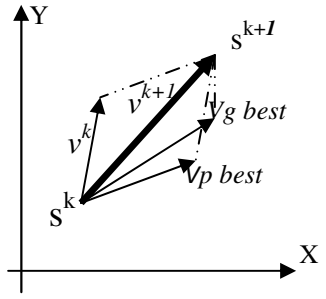

Fig.1: Principle of particle swarm method

B. Fitness Function

For searching an optimized size of the feature vector based on PSO algorithm, a fitness function is needed. In this work, we consider the variance calculated for every size of the feature vector as the fitness for this size and the goal is to optimize this fitness.

IV. CALCULATION PROCEDURE

The procedure of calculation consists of two main parts, the first part involves the extraction of relevant points from the radial vibration signals and their arrangement in vectors called feature vectors. This extraction is carried out by the RTF [24]. Since not all of the vector points are interesting, we proceed to the optimization of the vector using the PSO algorithm. Finally, only the first values are retained, the values that possess larger Fisher contrasts. The signals recorded by the acquisition system via three accelerometers are: the axial, radial and vertical vibration signals. In practice, the vibration signals have very low values; we conduct a priori preprocessing of the vibration data.

V. Experiment Results

The experimental data are collected at Ampère Laboratory, University of Lyon1. The experimental bench shown in Fig. 2 consists of a three-phase squirrel cage induction-motor Leroy Somer LS 132S, IP 55, Class F, T °C standard = 40 °C. The motor is loaded with a powder brake. Its maximum torque (100 Nm) is reached at rated speed.

This brake is sized to dissipate a maximum power of 5kW. The wear obtained on the bearings is a real one (Fig. 3).

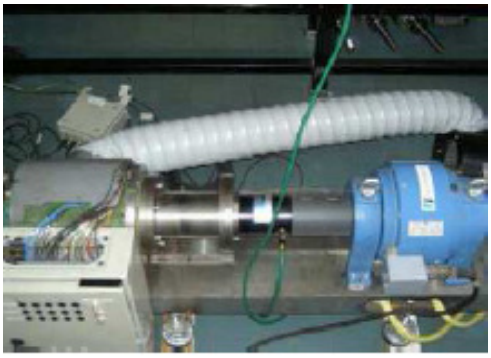

Fig. 2: The 5.5 kW motor coupled with load (powder brake).

Fig. 4 shows the device in place for the acquisition of signals: machine set up and acquisition of signals. The vibration signals sampling rate is 20 kHz. The number of samples per signal rises to *N*=100000 samples on an acquisition period of 5s. The data acquisition set consists of vibration signal recording at different levels of load (0%, 25%, 50%, 75% and 100%). Different operating conditions for the machine were considered, namely: healthy, bearing fault… etc.

Fig. 3: Accelerated wear of the bearings by immersion in acid

Each signal is sampled at a downsampling rate of 50. Only the range of the required frequencies is preserved, hence, the signal dimension is greatly reduced.

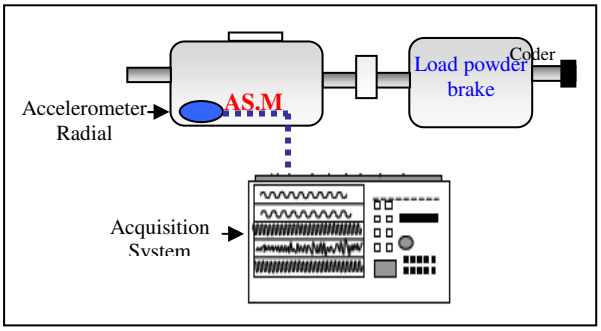

Fig.4: Signal Acquisition System

The dimension of ambiguity plane is 200×200 = 40000 points; by considering symmetry compared to the origin, we retain only the quarter of ambiguity plane, which corresponds to N = 10000. Figures 5, 6, 7 and 8 represent examples of RVAS for healthy and faulted machines. At the first glance, these figures do not exhibit any interesting feature. From these representations, we cannot extract any relevant information. For this reason, we proceed to the pre-processing of data and use of additional calculation methods mentioned below.

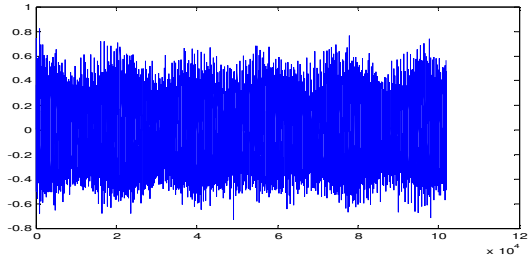

Fig.5: Radial vibration signal of a healthy 0% loaded machine

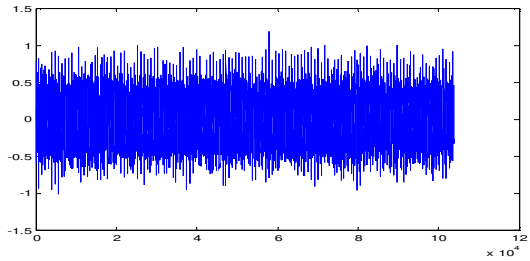

Fig. 6: Radial vibration signal of a healthy 75% loaded machine

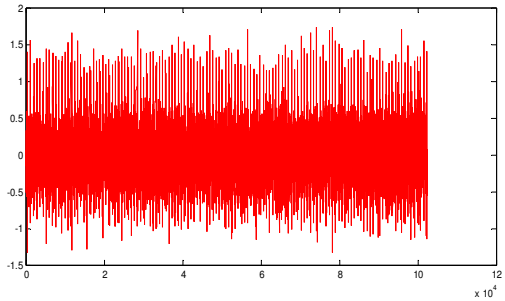

Fig. 7: Radial vibration signal of a 0% loaded bearing faulted machine

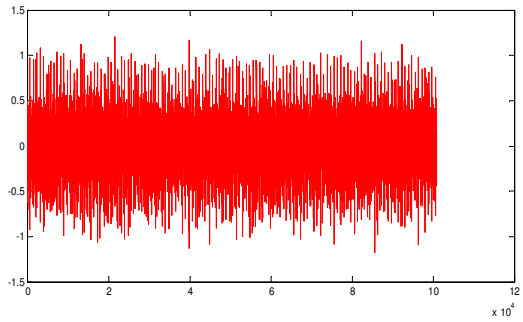

Fig. 8: Radial vibration signal of a 75% loaded bearing faulted machine

Figure 9 shows a representation of the cloud dispersion of the RVAS points of a healthy and bearing faulted machines for different levels of load (0%, 25%, 50%, 75%, 100%).

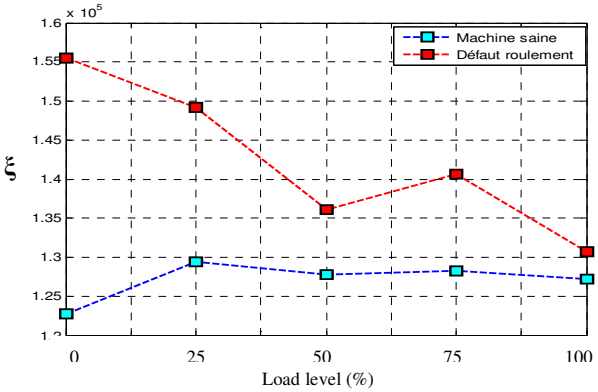

Fig. 9: Cloud dispersions of the RVAS.

We note in Figure 9 that the parameter ξ confirms the separability between two classes (healthy bearing class and faulty bearing class). We also note that the parameter ξ is not very sensitive to changes in the level of charge.

In this section we present the severity as a function of time and frequency for the radial vibrations for different load levels.

In this work, the objective of introducing the PSO is the optimization of the feature vectors size, by considering the variance as fitness function. Before the optimization procedure, the 10 feature vectors consisted of 10 elements. Using the PSO, the sizes of these vectors are reduced to 2 elements for each vector. Figures 10, 11 and 12 show the optimized feature vectors.

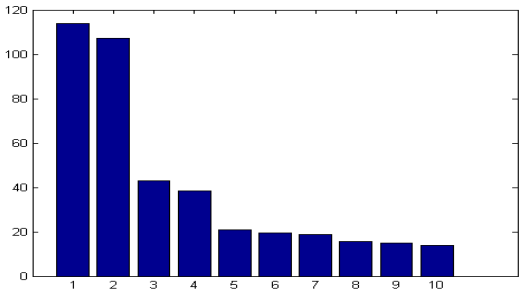

Fig10 : Optimized feature vector1

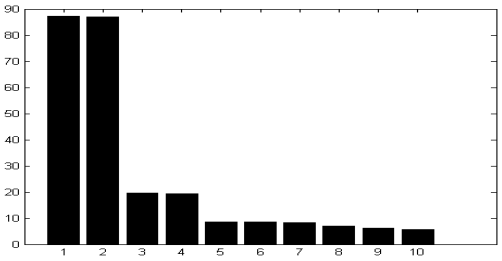

Fig11 : Optimized feature vector2

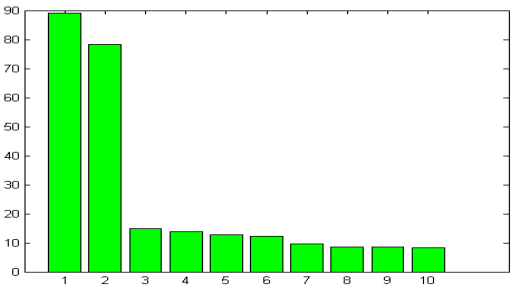

Fig12 : Optimized feature vector3

VI. Conclusion

In this paper, we have proposed a new method for fault diagnosis of induction machine based on the analysis of the radial vibration signal. Before the extraction of the feature vectors using the TFR_{SCD}, a data preprocessing is needed due to the low values of the vibration signal. This method involves the introduction of the cloud points dispersion parameter ξ, that calculates the Signal Class Dependent Time Frequency Representation "TFR_{SCD}" and the extraction of the feature vectors. We have introduced the PSO algorithm to optimize the sizes of the feature vectors. Since the sizes of the feature vectors are dramatically reduced to two points, this will significantly help optimize calculation time.

References

[1] P. J. Tavner, B. G. Gaydon, and D. M. Ward, "Monitoring Generators and Large Motors," *Proc. Inst. Elect. Eng.—B*, vol. 133, no. 3, pp. 169–180, May 1986.

[2] Wei, Qin; Yu, Fan; Jin, Fang"Characteristic and magnetic field analysis of a high temperature superconductor axial-flux coreless induction maglev motor" Journal of Applied Physics, Volume: 111, Issue: 7, 2012.

[3] Bouzid, M.; Champenois, G.; Bellaaj, N.M.; Signac, L.; Jelassi, K. "An Effective Neural Approach for the Automatic Location of Stator Interturn Faults in Induction Motor" IEEE Transactions on Industrial Electronics ,Vol 55 (12) pp 4277 – 4289,2008 .

[4] Filippetti, F.; Franceschini, G.; Tassoni, C."Neural networks aided on-line diagnostics of induction motor rotor faults" IEEE Transactions on Industry Applicationsl Vol 31(4) pp 892 – 899 1995.

[5] Cupertino, F.; Giordano, V.; Mininno, E.; Salvatore, L "Application of Supervised and Unsupervised Neural Networks for Broken Rotor Bar Detection in Induction Motors " IEEE International Conference on Electric Machines and Drives, pp 1895 – 1901 ,2005.

[6] Ghate, V.N. Dudul, S.V. " Fault Diagnosis of Three Phase Induction Motor Using Neural Network Techniques" 2nd International Conference on Emerging Trends in Engineering and Technology (ICETET), pp 922 - 928 ,16-18 Dec. 2009.

[7] Chow, M.-y.; Mangum, P.M.; Yee, S.O."A neural network approach to real-time condition monitoring of induction motors" IEEE

Transactions on Industrial Electronics l vo 38 (6)pp 448 – 453, 1991.

[8] H. Su and K. T. Chong, "Induction Machine Condition Monitoring Using Neural Network Modeling," *IEEE Trans. Ind. Electron.*, vol. 54, no. 1, pp. 241–249, Feb. 2007.

[9] Laala, W.; Guedini, S.; Zouzou, S. "Novel approach for diagnosis and detection of broken bar in induction motor at low slip using fuzzy logic", (SDEMPED), IEEE International Symposium on Diagnostics for Electric Machines, Power Electronics & Drives pp 511 – 516, 2011.

[10] A. Ordaz-Moreno, R. de Jesus Romero-Troncoso, J. A. Vite-Frias, J. R. Rivera-Gillen, and A. Garcia-Perez, "Automatic Online Diagnosis Algorithm for Broken-Bar Detection on Induction Motors Based on Discrete Wavelet Transform for FPGA Implementation" , *IEEE Trans. Ind. Electron.*, vol. 55, no. 5, pp. 2193–2202, May 2008.

[11] B. Yazıcı and G. B. Kliman, "An Adaptive Statistical Time–Frequency Method For Detection of Broken Bars and Bearing Faults in Motors Using Stator current," *IEEE Trans. Ind. Appl.*, vol. 35, no. 2, pp. 442–452, Mar./Apr. 1999.

[12] M. Wang, G. I. Rowe, and A. V. Mamishev, "Classification of Power Quality Events Using Optimal Time–Frequency Representations—Part 2: Application," *IEEE Trans. Power Del.*, vol. 19, no. 3, pp. 1496–1503, Jul. 2004.

[13] B. W. Gillespie and L. Atlas, "Optimizing Time–Frequency Kernels for Classification," *IEEE Trans. Signal Process.*, vol. 49, no. 3, pp. 485–496, Mar. 2001.

[14] J. Kennedy and R. Eberhart, "Particle swarm optimization," in Proc.IEEE Int. Conf. Neural Netw., vol. 4, Nov. 1995, pp. 1942–1948.

[15] P. J. Angeline, Using Selection to Improve Particle Swarm Optimization, in Proc. IEEE International Conference on Evolutionary. Computations, pp. 84–89, May 1998.

[16]J. Kennedy and R. Eberhart, Particle swarm optimization, Proc. IEEE Int. Conf. Neural Networks, Vol. IV, pp. 1942–1948, 1995.

Online fault detection of induction motors using frequency domain independent components analysis

[17] A. Lebaroud and G. Clerc, "Classification of Induction Machine Faults by Optimal Time frequency Representations," *IEEE Trans. on Industrial Electronics,* vol. 55, no. 12, december 2008.

[18] A. Lebaroud and G. Clerc, "Accurate Diagnosis of Induction Machine Faults Using Optimal Time–Frequency Representations" *Engineering Applications of Artificial Intelligence.* Vol. 22, Issues 4-5, June 2009, Pages 815-822.

[19] V. Rashtchi, R. Aghmasheh "A New Method for Identifying Broken Rotor Bars in Squirrel Cage Induction Motor Based on Particle Swarm Optimization Method ," World Academy of Science, Engineering and Technology Vol 67, pp. 694-698, 2010.

[20] J. Kennedy and R. Mendes, "Neighborhood topologies in fullyinformed and best-of-neighborhood particle swarms," Proc. of the IEEE International Workshop, pp. 45-50, June 2003.

[21] M'hamed, B. "Using Two Pso-Structures Approaches To Estimate Induction Machine Parameters ",13th European Conference on PowerElectronics and Applications,pp1-8 , 8-10 Sept. 2009.

[22] Hamid, R.H.A.; Amin, A.M.A.; Ahmed, R.S.; El-Gammal, A." New Technique for Maximum Efficiency and Minimum Operating Cost of Induction Motors Based on Particle Swarm Optmization (PSO) " IEEE International Symposium on Industrial Electronics , Vol: 3(21) pp 2176 - 2181 , : 2006.

[23] Fausett L. ''Fundamentals of neural networks architectures, algorithms, and applications.'' Englewo od Cliffs, NJ: Prentice Hall; 1994.

[24] A.Medoued, A.Lebaroud, A.Boukadoum, T.Boukra, G. Clerc, "Back Propagation Neural Network for Classification of Induction Machine Faults," 8th SDEMPED, IEEE Symposium on Diagnostics for Electrical Machines, Power Electronics & Drives September 5-8, 2011, Bologna, Italy, pp 525-528, 2011.